Intermetallics 183 (2025) 108809

Contents lists available at ScienceDirect

Intermetallics

journal homepage: www.elsevier.com/locate/intermet

Development of new all–metal FeCoZrAl amorphous alloys for room–temperature magnetic refrigeration application

Xueru Fan [a,b], Hangboce Yin [d], Qiang Li [c,*], Juntao Huo [d,**], Chuntao Chang [e,***]

[a] School of Physics Science and Technology, Xinjiang University, Urumqi, Xinjiang, 830046, People's Republic of China
[b] Xinjiang Key Laboratory of Solid State Physics and Devices, Xinjiang University, Urumqi, Xinjiang, 830046, People's Republic of China
[c] School of Materials Science and Engineering, Xinjiang University, Urumqi, Xinjiang, 830046, People's Republic of China
[d] CAS Key Laboratory of Magnetic Materials and Devices, and Zhejiang Province Key Laboratory of Magnetic Materials and Application Technology, Ningbo Institute of Materials Technology and Engineering, Chinese Academy of Sciences, Ningbo, 315201, People's Republic of China
[e] School of Mechanical Engineering, Neutron Scattering Technical Engineering Research Center, Dongguan University of Technology, Dongguan, Guangdong, 523808, People's Republic of China

ARTICLE INFO

Keywords:
All–metal Fe–based amorphous alloy
High Fe content
Room–temperature magnetic refrigeration
Magnetocaloric effect

ABSTRACT

This study introduces the development of a novel, all–metal $Fe_{88}Co_4Zr_7Al_1$ amorphous alloy designed for room–temperature magnetic refrigeration application, highlighting the potential of all–metal Fe–based amorphous alloys in magnetic refrigeration applications. By innovatively adjusting the Curie temperature and enhancing the saturation magnetic flux density through Co addition, this work pioneers a strategy to develop all–metal Fe–based amorphous alloys with room–temperature magnetocaloric effect, historically focused on Fe–metalloid configurations with limited breakthroughs. The all–metal $Fe_{88}Co_4Zr_7Al_1$ amorphous alloy, synthesized via a melt–spinning technique, demonstrates exceptional magnetocaloric effect properties, including a Curie temperature of 303 K, a maximum isothermal magnetic entropy change of 3.23 J $kg^{-1}\cdot K^{-1}$, and the refrigerant capacity of 650 J kg^{-1} under an applied magnetic field change of 5 T. These properties, combined with negligible hysteresis loss and lower costs due to the absence of rare earth elements, position the alloy as a promising candidate for room–temperature magnetic refrigerants.

1. Introduction

Magnetic refrigeration is a newly developed refrigeration technology and is regarded as a promising alternative for the traditional vapor–cycle refrigeration [1]. Due to the great advantages such as environmental friendliness and relatively high efficiency than the traditional vapor expansion–compression cycle, room temperature magnetic refrigeration technology based on the magnetocaloric effect (MCE) has attracted intense research interest [2–4]. Therefore, experts working on the magnetic cooling technology have paid more attentions in recent years on the novel magnetocaloric materials that can be applied as magnetic refrigerants near the ambient temperature. To date, several intermetallic compounds, such as Gd–Si–Ge [5], La–Ca–Mn–O [6], Ni–Mn–Ga [7], La–Fe–Si [8], Mn–Fe–P–As [9], Ni–Mn–Sn [10], have been found to exhibit a giant MCE based on the first–order magnetic phase transitions (FOMT). However, the inherent large thermal and magnetic hysteresis associated with FOMT limits the operational frequency and refrigeration efficiency of these materials in refrigeration applications [11]. In contrast, amorphous alloys as magnetic refrigeration materials, characterized by second–order magnetic phase transformations (SOMT), present superior attributes over FOMT materials. These include small magnetic and thermal hysteresis, an expansive working temperature span, enhanced refrigeration capacity (RC), elevated electrical resistivity, corrosion resistance, and the capability to adjust the transition temperature through alloying [12–15].

The quest for efficient room–temperature refrigeration is critical due to its vast potential in civilian applications. Amorphous alloys, pivotal in magnetic refrigeration, can be broadly categorized into rare–earth–metal (RE) based and transition–metal (TM) based varieties. RE–based amorphous alloys, including Gd– [16–18], Tb– [19], and

* Corresponding author.
** Corresponding author.
*** Corresponding author.
E-mail addresses: qli@xju.edu.cn (Q. Li), huojuntao@nimte.ac.cn (J. Huo), changct@dgut.edu.cn (C. Chang).

https://doi.org/10.1016/j.intermet.2025.108809
Received 24 January 2025; Received in revised form 25 March 2025; Accepted 22 April 2025
Available online 24 April 2025

Dy–based [20], are distinguished by their exceptional magnetic entropy change and refrigeration capacity at lower temperatures. However, these alloys exhibit diminishing magnetocaloric properties as their Curie temperatures (T_c) are adjusted towards room temperature, alongside the drawback of high raw material costs. In contrast, TM–based amorphous alloys are more economically viable, offering a wide range of composition adjustments. Their T_c can be readily modified to desired levels through the incorporation of other elements, without significantly compromising their beneficial MCE [21–25]. Unfortunately, $|\Delta S_M^{max}|$ of these TM–based amorphous alloys is insufficient for their application in magnetic refrigerator. Therefore, low cost amorphous magnetic refrigerants with improved formability $|\Delta S_M^{max}|$ and appropriate T_c are essential for the commercial application of these alloys in domestic magnetic refrigerators.

Recent years have witnessed the development of numerous multi-component amorphous alloys with room–temperature MCE, particularly within the Fe–Zr–B system (Nanoperm–type) [4,25–32]. Introducing antiferromagnetic or paramagnetic elements (Mn, Cr, Zr, Nb, Ta, etc.) into Fe–Zr–B amorphous alloys can depress T_c close to room temperature, enabling near room–temperature MCE [12,22,25,26,30–32]. However, these alloys exhibited a modest MCE at room temperature. To enhance both the MCE and RC, rare earth elements with significant atomic magnetic moments (e.g., La, Ce, Sm, and Gd) are incorporated into Fe–Zr–B amorphous alloys [23,33–35]. However, the addition of rare earth elements increases the viscosity of the alloy melt and the risk of reaction with the crucible, making complicating sample preparation. More recently, a novel high Fe content $Fe_{83}Mo_6Si_1B_7P_2C_1$ amorphous alloy with a room–temperature MCE had been developed, demonstrating relatively high MCE and RC, attributable to its high Fe content [36]. Despite these advancements, significant progress in this domain remains limited, with the focus primarily on Fe–metalloid (Si, B, P, and C) type amorphous alloys. However, the addition of excessive metalloid elements can have significant negative effects on the properties of amorphous alloys [3,24,36], such as reducing soft magnetic properties and increasing alloy brittleness, thereby affecting the material's work-ability and practicality. Especially in the pursuit of high saturation magnetization alloy design, when the Fe content exceeds 85 at. %, the amorphous formation ability of the material has approached its theoretical limit [3], which poses significant challenges for alloy design. Compared with Fe–metalloid (Si, B, P, and C) type amorphous alloys, all metal Fe–based amorphous alloys exhibit superior toughness and plasticity due to their metal bonding characteristic [37], which will be more conducive to expanding their application fields. Recently, Yang [38] reported an all metal $Fe_{91-x}Zr_9Cu_x$ amorphous alloys showing promising MCE at low temperatures, yet their T_c is well below room temperature, rendering them unsuitable for ambient–temperature applications.

In the present work, we have developed an innovative all–metal $Fe_{88}Co_4Zr_7Al_1$ amorphous alloy, which exhibits an outstanding MCE at room temperature, surpassing the performance of existing Fe–based amorphous alloys in this regard. The findings of this work are expected to provide valuable insights and serve as a foundational guide for the development of novel amorphous alloys with room–temperature MCE.

2. Experiment procedures

Ingots with nominal compositions of $Fe_{92-x}Co_xZr_7Al_1$ (x = 0, 3, 4 and 5 at. %) were synthesized by arc melting the mixture of pure metals (99.99 wt %) in a Ti-gettered argon atmosphere. To ensure homogeneity, each ingot was remelted five times. Amorphous ribbons, approximately 1 mm in width and 25 μm in thickness, were fabricated via the single–roller melt–spinning method with a surface speed of 50 m/s under an argon atmosphere.

The amorphous nature of the melt–spun ribbons was verified by X–ray diffraction (XRD, Bruker D8 advance diffractometer) with Cu K_α radiation. Thermal analysis was performed using a differential scanning calorimeter (DSC, 404 C, Netsch) at a heating rate of 40 K/min. The temperature and field dependences of the DC magnetization of the samples were measured using a superconducting quantum magnetometer (SQUID, MPMS XL–7). The temperature dependence of the magnetization (M–T) of the samples was measured under a field of 200 Oe in the temperature range of 100–400 K. The isothermal magnetization (M − H) curves were acquired at various temperatures under a maximum field of 5 T. The isothermal magnetic entropy change versus temperature (ΔS_M–T) curve under different applied fields was derived from the isothermal magnetization data at different temperatures using the Maxwell relation [39]. The RC is defined as the product of the half–peak width of the ΔS_M curve and the peak ΔS_M for the samples [40].

3. Result and discussion

Fig. 1 presents the XRD patterns and the DSC curves of as–quenched (AQ) $Fe_{92-x}Co_xZr_7Al_1$ (x = 0, 3, 4 and 5 at. %) ribbons. As shown in Fig. 1 (a), there are only broad halo peak without sharp diffraction peak of crystallization in the XRD patterns of all the samples, revealing a fully amorphous nature. Fig. 1(b) displays the thermal scan curves of the AQ ribbon samples. The multiple distinct exothermic peaks can be observed in each DSC curve, which further confirms the glassy nature of the samples.

Fig. 2 (a) shows the hysteresis loop of the AQ $Fe_{92-x}Co_xZr_7Al_1$ (x = 0, 3, 4 and 5 at. %) amorphous ribbons at a temperature of 10 K. The M_s of the FeCoZrAl amorphous ribbons monotonously increases from 117.3 to 151.5 emu/g with the increase of Co content from 0 to 5 at. %, indicating the excellent soft magnetic properties. Fe–based amorphous alloys are

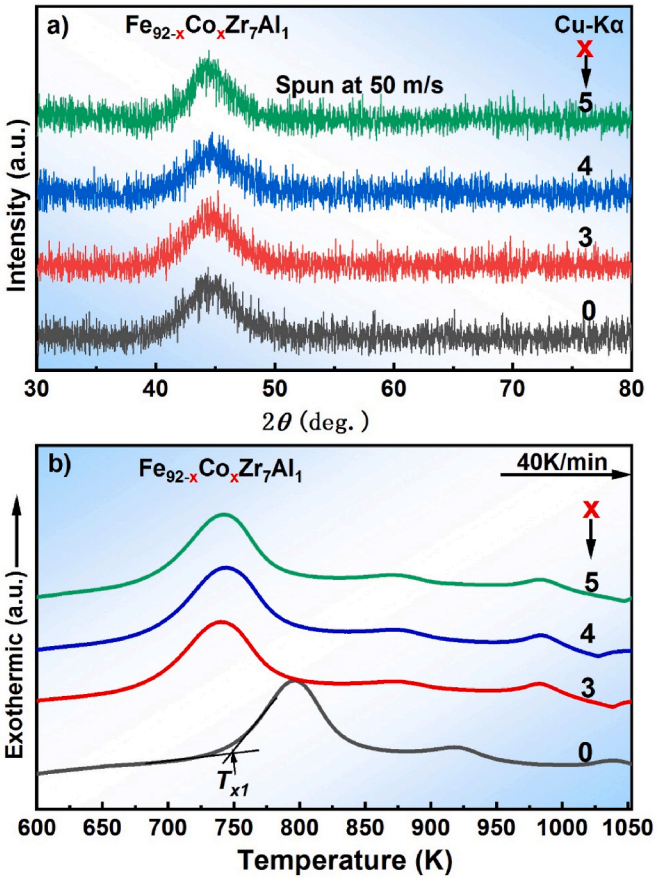

Fig. 1. (a) The XRD pattern of $Fe_{92-x}Co_xZr_7Al_1$ (x = 0, 3, 4 and 5 at. %) amorphous alloy ribbons; (b) DSC thermodynamic scanning curve at the heating rate of 40 K/min.

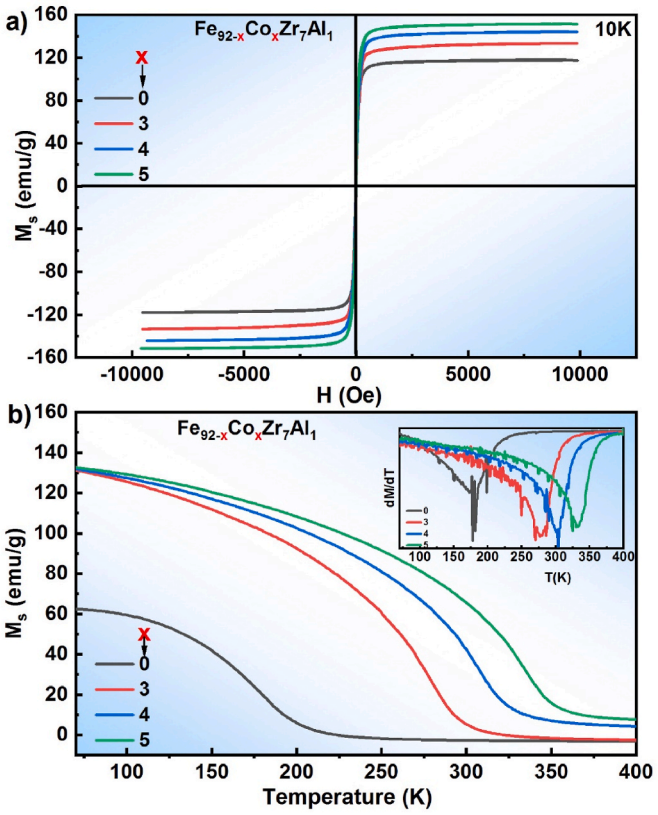

Fig. 2. (a) Hysteresis loops at a temperature of 10 K for the AQ $Fe_{92-x}Co_xZr_7Al_1$ (x = 0, 3, 4 and 5 at.%) amorphous alloy ribbons; (b) $M - T$ curves and the corresponding $dM/dT - T$ curves (inset) under an applied field of 200 Oe.

generally considered as weak ferromagnetism, i.e., both spin–up and spin–down bands are partially filled at the Fermi energy [13] Based on the band–gap theory [41], the state density of the spin–up band reaches the maximum while that of the spin–down band reaches the minimum near the Fermi level for the ferromagnetic materials. Co atom has more 3d electrons than Fe atom, and so the number of electrons occupying the spin–up band increases more than the spin–down band as Co gradually replaces Fe in Fe–based amorphous alloys. As a result, the magnetic moment per magnetic atom of the present FeCoZrAl amorphous alloys increases with a small amount of Fe replaced by Co.

Fig. 2 (b) shows the M–T curves and dM/dT–T curves (inset) of the AQ $Fe_{92-x}Co_xZr_7Al_1$ (x = 0, 3, 4 and 5 at. %) amorphous ribbons under an applied magnetic field of 200 Oe in the temperature range of 100–400 K. The T_c of the $Fe_{92-x}Co_xZr_7Al_1$ amorphous alloys can be determined from dM/dT–T curve to be 178.5 K, 279.5 K, 303.0 K and 333.4 K for x = 0, 3, 4 and 5, respectively. It can see that the T_c of the present all–metal Fe–based amorphous alloys increases with the Co content. Based on the mean field theory [42], the T_c is proportional to the exchange integral and the average spin moment of magnetic atoms, i.e. the saturation magnetization. The exchange integral strongly depends on the nearest distance between magnetic atoms. Based on the well–known Bethe–Slater curve [42], it may expect that the substitution of Co for Fe will lead to the increased average atomic diameter [43] and thus the stronger atomic exchange interaction. As a consequence, the average atomic exchange interaction between magnetic atoms becomes stronger with the increase of the substitution of Co for Fe. Meanwhile, it is also shown from Fig. 2 (a) that the saturation magnetization of the specimens monotonously increases with the Co content. Thus the T_c monotonously rises with increased Co substitution in the present FeCoZrAl amorphous alloys. The similar results are also found in other reported studies [44]. It is also noted that the $Fe_{88}Co_4Zr_7Al_1$ amorphous ribbon has a near room temperature T_c of 303.0 K and thus its magnetocaloric properties will be further investigated in detail below.

Fig. 3(a) shows the isothermal magnetization curves of the $Fe_{88}Co_4Zr_7Al_1$ amorphous ribbon, in which the applied magnetic field varies from 0 to 5 T and the measured temperature ranges from 100 K to 400 K. It can be seen that the magnetization of the sample achieves saturation at low applied magnetic fields when the measured temperature is below T_c, while the M − H curves of the sample become linear when the measured temperature is near and above T_c, indicating the transition behavior from ferromagnetic state to paramagnetic state. In order to understand the type of magnetic transition, the Arrott plots of the $Fe_{88}Co_4Zr_7Al_1$ amorphous ribbon derived from the M − H curve are shown in Fig. 3(b). The positive slopes indicate that the magnetic transitions in the $Fe_{88}Co_4Zr_7Al_1$ amorphous ribbon are of second order magnetic transition in nature [45]. In addition, the non–hysteresis phenomenon in SOMT can reduce the magnetic loss, which offers the possibility of it being a potential magnetic refrigeration material [46].

The magnetic entropy change (ΔS_M) is an essential parameter for characterizing the MCE of magnetocaloric materials. According to Maxwell's equations, the ΔS_M of the studied materials is calculated using the following equation [47]:

$$\Delta S_M(T, H_{max}) = \frac{\int_0^{H_{max}} M(T_i, H)dH - \int_0^{H_{max}} M(T_{i+1}, H)dH}{T_i - T_{i+1}} \quad (1)$$

Where H_{max} is the maximum applied field. By calculating the isothermal M − H curves of the $Fe_{88}Co_4Zr_7Al_1$ amorphous ribbon at different temperatures as shown in Fig. 3(a), the $(-\Delta S_M)$–T relationship at various maximum magnetic fields is presented in Fig. 4. It can be seen from Fig. 4 that the ΔS_M of the $Fe_{88}Co_4Zr_7Al_1$ amorphous ribbon increases with the maximum applied magnetic field, and the peak value ($|\Delta S_M^{max}|$) of the $(-\Delta S_M)$–T curves is around T_c. $|\Delta S_M^{max}|$ and RC of the $Fe_{88}Co_4Zr_7Al_1$ amorphous ribbon under the applied field of 2 T and 5 T are about 1.45 J $kg^{-1}\cdot K^{-1}$ and 268 J kg^{-1}, and 3.23 J $kg^{-1}\cdot K^{-1}$and 650 J kg^{-1}, respectively. The $|\Delta S_M^{max}|$ and RC under the applied field of 2 T and 5 T of the $Fe_{88}Co_4Zr_7Al_1$ amorphous ribbon together with some selected Fe–based and Co–based amorphous alloys with near room temperature

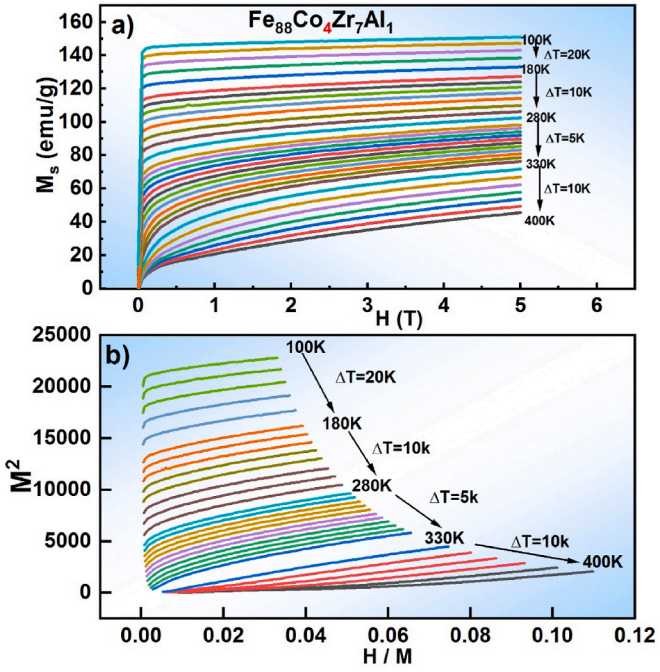

Fig. 3. M − H curves (a) and Arrott plots (b) of the $Fe_{88}Co_4Zr_7Al_1$ amorphous ribbon measured at various temperatures under the maximum applied field of 5 T.

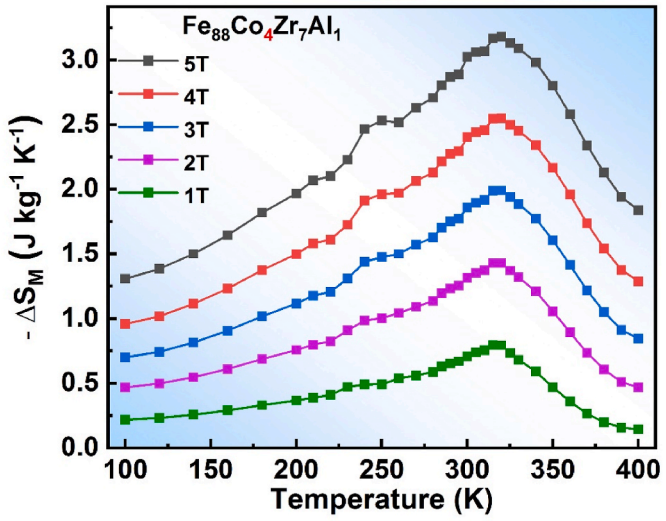

Fig. 4. The ($-\Delta S_M$)–T curves of the $Fe_{88}Co_4Zr_7Al_1$ amorphous ribbon under the magnetic field changes of 1, 2, 3, 4 and 5 T.

MCE are summarized in Table 1 and present in Fig. 5. It can be seen that the present $Fe_{88}Co_4Zr_7Al_1$ amorphous alloy has relatively large values of $|\Delta S_M^{max}|$ and RC among these amorphous alloys with near room–temperature MCE. It can also be noted that, compared with the Fe–metalloid type amorphous alloy, the present all–metal $Fe_{88}Co_4Zr_7Al_1$ amorphous alloy has a larger RC, which is due to its wide magnetic transition temperature range. Moreover, the present $Fe_{88}Co_4Zr_7Al_1$ amorphous alloy does not contain any rare earth elements and thus has the advantage of low cost.

According to the mean–field theory, the relationship between $|\Delta S_M^{max}|$ and the magnetic field (H) is $|\Delta S_M^{max}| \propto H^n$ [50]. By fitting the experimental data in Fig. 6 with the above relationships, the value of the exponent *n* for the $Fe_{88}Co_4Zr_7Al_1$ amorphous ribbon is 0.86, which deviates greatly from the value of 2/3 predicted by the mean field theory [42], implying the existence of fluctuations and inhomogeneity in the magnetic microstructure [48], which may be responsible for the wide magnetic transition temperature range of the present all–metal Fe–based amorphous alloys.

It is known that the value of $|\Delta S_M^{max}|$ an alloy is proportional to its M_s [40]. The plot of M_s against $|\Delta S_M^{max}|$ under the applied magnetic field of 5 T for the present $Fe_{88}Co_4Zr_7Al_1$ and some TM–based amorphous alloy

Table 1
Magnetocaloric properties of the present $Fe_{88}Co_4Zr_7Al_1$ amorphous alloy and some several reported Fe–based amorphous alloys with near room–temperature MCE.

No.	Composition (at. %)	T_c (K)	$\|\Delta S_M^{max}\|$ ($J \cdot kg^{-1} \cdot K^{-1}$)		RC ($J \cdot kg^{-1}$)		Ref.
			2T	5T	2T	5T	
1	$Fe_{88}Co_4Zr_7Al_1$	303	1.45	3.20	268	~650	This work
2	$Fe_{88}Zr_9B_3$	286	1.59	3.17	/	/	[24]
3	$Fe_{87}Zr_9B_4$	304	1.67	3.29	/	/	[24]
4	$Fe_{88}Zr_8B_4$	280	1.3	2.8	201	551	[30]
5	$Fe_{87}Co_1Zr_8B_4$	317	1.61	3.24	/	/	[23]
6	$Fe_{87}Zr_6B_6Cu_1$	300	1.6	3.0	208	590	[31]
7	$Fe_{86}Zr_7B_6Cu_1$	320	1.6	3.1	205	582	[30]
8	$Fe_{75}Ta_5Zr_9B_{10}Cu_1$	313	1.04	2.03	92.2	241.5	[32]
9	$Fe_{87}Zr_8B_4Sm_1$	308	1.65	3.27	/	/	[23]
10	$Fe_{86}La_7Ce_2B_5$	313	/	3.64	/	/	[33]
11	$Fe_{88}La_4Ce_3B_5$	303	1.54	3.93	201	715.3	[33]
12	$Fe_{83}Mo_6Si_1B_7P_2C_1$	300	1.06	2.74	138.2	485.2	[36]
13	$Co_{71}Mo_9P_{14}B_6$	317	0.47	0.96	41.3	70.5	[48]
14	$Fe_{71}Cr_7Si_4Nb_5B_{12}Ag_1$	300	/	2.1	/	/	[49]

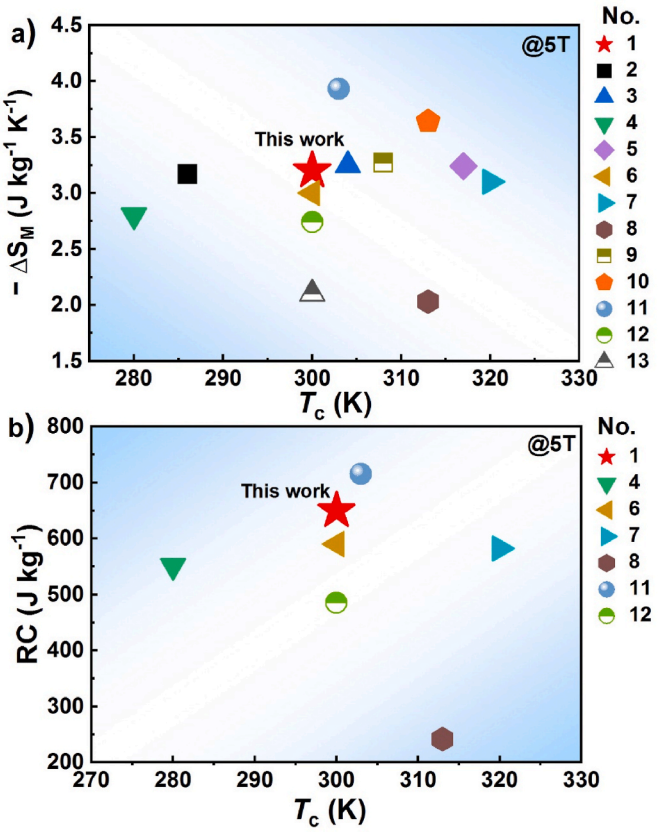

Fig. 5. Comparisons of (a) the maximum magnetic entropy change ($|\Delta S_M^{max}|$) and (b) refrigerant capacity (RC) for the $Fe_{88}Co_4Zr_7Al_1$ and other metallic glasses listed in Table 1.

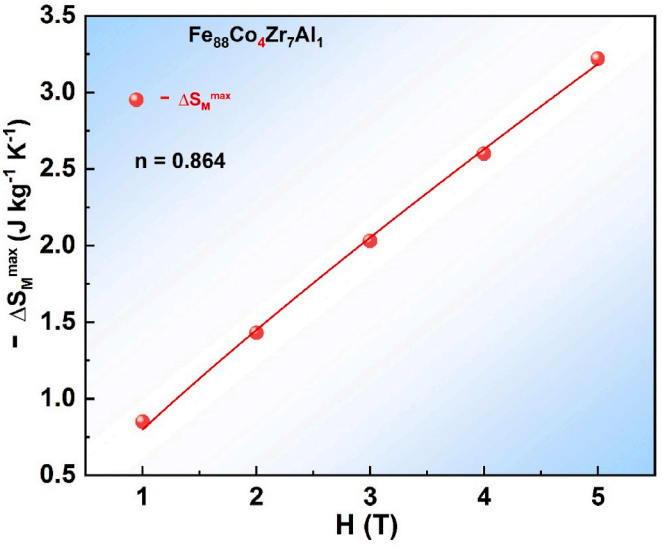

Fig. 6. (a) Magnetic field dependence of the maximum magnetic entropy changes ($|\Delta S_M^{max}|$) for the $Fe_{88}Co_4Zr_7Al_1$ amorphous ribbon.

is shown in Fig. 7. The data points corresponding to these TM–based amorphous alloy are linearly fitted by the least squares method and the R–square of the fitted straight line is 0.987, indicating a good linear relationship between the M_s and $|\Delta S_M^{max}|$. The present $Fe_{88}Co_4Zr_7Al_1$ amorphous alloy also follows this linear relationship, suggesting that the present all–metal Fe–based amorphous alloy has a similar MCE

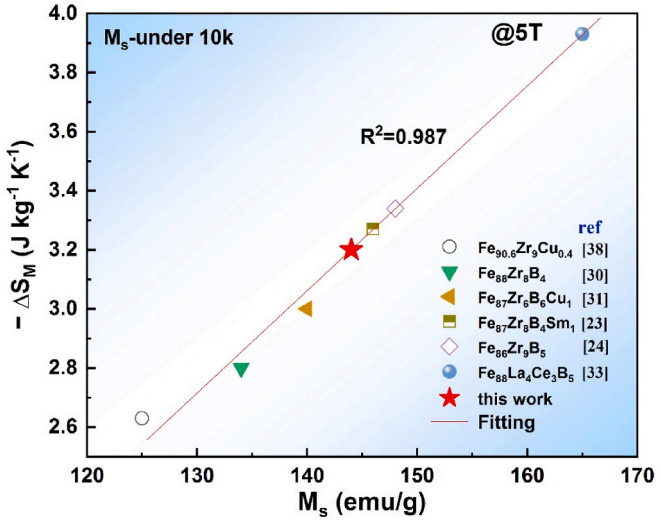

Fig. 7. Plot of saturation magnetization against the maximum magnetic entropy change ($|\Delta S_M^{max}|$) of the present $Fe_{88}Co_4Zr_7Al_1$ and other metallic glasses under the applied magnetic field of 5 T.

mechanism to Fe–metalloid type amorphous alloys.

4. Conclusion

This study successfully demonstrates the development and characterization of an innovative all–metal $Fe_{88}Co_4Zr_7Al_1$ amorphous alloy, tailored for room–temperature magnetic refrigeration applications. The $Fe_{88}Co_4Zr_7Al_1$ amorphous alloy ribbon exhibits a T_c of 303 K, a M_s of 144 emu/g, a $|\Delta S_M^{max}|$ of 3.23 J kg^{-1}·K^{-1} and a RC of 650 J kg^{-1} under an applied field of 5 T. In comparison to existing Fe–based amorphous alloys known for their near room–temperature MCE, the all–metal $Fe_{88}Co_4Zr_7Al_1$ amorphous alloy stands out not only for its superior magnetocaloric performance but also for its composition, which is devoid of rare–earth and metalloid elements, thereby ensuring both superior magnetocaloric properties and cost–effectiveness. This work has opened up new avenues for the development of novel room–temperature magnetic refrigeration materials.

CRediT authorship contribution statement

Xueru Fan: Writing – original draft. **Hangboce Yin:** Writing – review & editing. **Qiang Li:** Writing – review & editing. **Juntao Huo:** Writing – review & editing. **Chuntao Chang:** Writing – review & editing.

Declaration of competing interest

The authors declare no conflict of interest in this paper.

Acknowledgements

This research was supported by National Natural Science Foundation of China (Grant Nos. 52261033 and 51771161).

Data availability

Data will be made available on request.

References

[1] J. Glanz, Making a bigger chill with magnets, Science 279 (5359) (1998) 2045, https://doi.org/10.1126/science.279.5359.2045, 2045.

[2] Q. Luo, B. Schwarz, N. Mattern, J. Shen, J. Eckert, Roles of hydrogenation, annealing and field in the structure and magnetic entropy change of Tb-based bulk metallic glasses, AIP Adv. 3 (3) (2013) 032134, https://doi.org/10.1063/1.4797619.

[3] O. Gutfleisch, M.A. Willard, E. Brück, C.H. Chen, S.G. Sankar, J.P. Liu, Magnetic materials and devices for the 21st century: stronger, lighter, and more energy efficient, Adv. Mater. 23 (7) (2011) 821–842, https://doi.org/10.1002/adma.201002180.

[4] V. Franco, J.S. Blázquez, B. Ingale, A. Conde, The magnetocaloric effect and magnetic refrigeration near room temperature: materials and Models, Annu. Rev. Mater. Res. 42 (1) (2012) 305–342, https://doi.org/10.1002/chin.201324197.

[5] V.K. Pecharsky, K.A. Gschneidner Jr., Giant magnetocaloric effect in $Gd_5(Si_2Ge_2)$, Phys. Rev. Lett. 78 (23) (1997) 4494–4497, https://doi.org/10.1103/PhysRevLett.78.4494.

[6] Z.B. Guo, Y.W. Du, J.S. Zhu, H. Huang, W.P. Ding, D. Feng, Large magnetic entropy change in perovskite-type manganese oxides, Phys. Rev. Lett. 78 (6) (1997) 1142–1145, https://doi.org/10.1103/PhysRevLett.78.1142.

[7] F. Hu, B. Shen, J. Sun, Magnetic entropy change in $Ni_{51.5}Mn_{22.7}Ga_{25.8}$ alloy, Appl. Phys. Lett. 76 (23) (2000) 3460–3462, https://doi.org/10.1063/1.126677.

[8] F. Hu, B. Shen, J. Sun, Z. Cheng, G. Rao, X. Zhang, Influence of negative lattice expansion and metamagnetic transition on magnetic entropy change in the compound $LaFe_{11.4}Si_{1.6}$, Appl. Phys. Lett. 78 (23) (2001) 3675–3677, https://doi.org/10.1063/1.1375836.

[9] O. Tegus, E. Brück, K.H.J. Buschow, F.R. de Boer, Transition-metal-based magnetic refrigerants for room-temperature applications, Nature 415 (6868) (2002) 150–152, https://doi.org/10.1038/415150a.

[10] Y. Zhang, Q. Zheng, W. Xia, J. Zhang, J. Du, A. Yan, Enhanced large magnetic entropy change and adiabatic temperature change of $Ni_{43}Mn_{46}Sn_{11}$ alloys by a rapid solidification method, Scripta Mater. 104 (2015) 41–44, https://doi.org/10.1016/j.scriptamat.2015.04.004.

[11] Y. Wang, X. Bi, The role of Zr and B in room temperature magnetic entropy change of FeZrB amorphous alloys, Appl. Phys. Lett. 95 (26) (2009) 262501, https://doi.org/10.1063/1.3276558.

[12] R. Caballero-Flores, V. Franco, A. Conde, K.E. Knipling, M.A. Willard, Influence of Co and Ni addition on the magnetocaloric effect in $Fe_{88-2x}Co_xNi_xZr_7B_4Cu_1$ soft magnetic amorphous alloys, Appl. Phys. Lett. 96 (18) (2010) 182506, https://doi.org/10.1063/1.3427439.

[13] S. Meng, H. Ling, Q. Li, J. Zhang, Development of Fe-based bulk metallic glasses with high saturation magnetization, Scripta Mater. 81 (2014) 24–27, https://doi.org/10.1016/j.scriptamat.2014.02.018.

[14] S.J. Pang, T. Zhang, K. Asami, A. Inoue, Synthesis of Fe–Cr–Mo–C–B–P bulk metallic glasses with high corrosion resistance, Acta Mater. 50 (3) (2002) 489–497, https://doi.org/10.1016/S1359-6454(01)00366-4.

[15] W. Yang, H. Liu, L. Xue, J. Li, C. Dun, J. Zhang, Y. Zhao, B. Shen, Magnetic properties of $(Fe_{1-x}Ni_x)_{72}B_{20}Si_4Nb_4$ (x=0.0–0.5) bulk metallic glasses, J. Magn. Magn Mater. 335 (2013) 172–176, https://doi.org/10.1016/j.jmmm.2013.02.004.

[16] N.S. Bingham, H. Wang, F. Qin, H.X. Peng, J.F. Sun, V. Franco, H. Srikanth, M. H. Phan, Excellent magnetocaloric properties of melt-extracted Gd-based amorphous microwires, Appl. Phys. Lett. 101 (10) (2012) 102407, https://doi.org/10.1063/1.4751038.

[17] X. Wang, B.Z. Tang, Q. Wang, P. Yu, D. Ding, L. Xia, $Co_{50}Gd_{48-x}Fe_2Ni_x$ amorphous alloys with high adiabatic temperature rise near the hot end of a domestic magnetic refrigerator, J. Non-Cryst. Solids 544 (2020) 120146, https://doi.org/10.1016/j.jnoncrysol.2020.120146.

[18] F. Yuan, Q. Li, B. Shen, The effect of Fe/Al ratio on the thermal stability and magnetocaloric effect of $Gd_{55}Fe_xAl_{45-x}$ (x = 15–35) glassy ribbons, J. Appl. Phys. 111 (7) (2012) 07A937, https://doi.org/10.1063/1.3677780.

[19] X. Wang, D. Ding, L. Cui, L. Xia, Compositional dependence of curie temperature and magnetic entropy change in the amorphous Tb–Co ribbons, Materials 14 (4) (2021) 1002, https://doi.org/10.3390/ma14041002.

[20] L.Y. Ma, B.Z. Tang, K.C. Chan, L. Zhao, M.B. Tang, D. Ding, L. Xia, Formability and magnetic properties of Dy-Co binary amorphous alloys, AIP Adv. 8 (7) (2018) 075215, https://doi.org/10.1063/1.5037357.

[21] I. Škorvánek, J. Kováč, J. Marcin, P. Švec, D. Janičkovič, Magnetocaloric effect in amorphous and nanocrystalline $Fe_{81-x}Cr_xNb_7B_{12}$ (x=0 and 3.5) alloys, Mater. Sci. Eng: A 449–451 (2007) 460–463, https://doi.org/10.1016/j.msea.2006.02.353.

[22] Y.K. Fang, C.C. Yeh, C.C. Hsieh, C.W. Chang, H.W. Chang, W.C. Chang, X.M. Li, W. Li, Magnetocaloric effect in Fe–Zr–B–M (M=Mn, Cr, and Co) amorphous systems, J. Appl. Phys. 105 (7) (2009) 07A910, https://doi.org/10.1063/1.3054369.

[23] L. Chen, J. Zhang, L. Wen, P. Yu, L. Xia, Outstanding magnetocaloric effect of $Fe_{88-x}Zr_8B_4Sm_x$ (x=0, 1, 2, 3) amorphous alloys, Sci. China Phys. Mech. Astron. 61 (5) (2018) 056121, https://doi.org/10.1007/s11433-017-9152-7.

[24] P. Yu, J.Z. Zhang, L. Xia, Effect of boron on the magneto-caloric effect in $Fe_{91-x}Zr_9B_x$ (x = 3, 4, 5) amorphous alloys, J. Mater. Sci. 52 (24) (2017) 13948–13955, https://doi.org/10.1007/s10853-017-1476-9.

[25] L. Gan, L. Ma, B. Tang, D. Ding, L. Xia, Effect of Co substitution on the glass forming ability and magnetocaloric effect of $Fe_{88}Zr_8B_4$ amorphous alloys, Sci. China Phys. Mech. Astron. 60 (7) (2017) 076121, https://doi.org/10.1007/s11433-017-9043-4.

[26] G.F. Wang, H.L. Li, Z.R. Zhao, X.F. Zhang, Stable magnetocaloric effect and refrigeration capacity in Co-doped FeCoMnZrNbB amorphous ribbons near room temperature, J. Alloys Compd. 692 (2017) 793–796, https://doi.org/10.1016/j.jallcom.2016.09.105.

[27] P. Álvarez, P. Gorria, J. Sánchez Marcos, L. Fernández Barquín, J.A. Blanco, The role of boron on the magneto-caloric effect of FeZrB metallic glasses, Intermetallics 18 (12) (2010) 2464–2467, https://doi.org/10.1016/j.intermet.2010.07.018.
[28] D. Mishra, M. Gurram, A. Reddy, A. Perumal, P. Saravanan, A. Srinivasan, Enhanced soft magnetic properties and magnetocaloric effect in B substituted amorphous Fe–Zr alloy ribbons, Mater. Sci. Eng: B 175 (3) (2010) 253–260, https://doi.org/10.1016/j.mseb.2010.07.038.
[29] V. Franco, J.S. Blázquez, A. Conde, The influence of Co addition on the magnetocaloric effect of Nanoperm-type amorphous alloys, J. Appl. Phys. 100 (6) (2006) 064307, https://doi.org/10.1063/1.2337871.
[30] P. Alvarez-Alonso, J.L. Sánchez Llamazares, C.F. Sánchez-Valdés, M.L. Fdez-Gubieda, P. Gorria, J.A. Blanco, High-magnetic field characterization of magnetocaloric effect in FeZrB(Cu) amorphous ribbons, J. Appl. Phys. 117 (17) (2015) 17A710, https://doi.org/10.1063/1.4907188.
[31] P. Álvarez, J.L. Sánchez Llamazares, P. Gorria, J.A. Blanco, Enhanced refrigerant capacity and magnetic entropy flattening using a two-amorphous FeZrB(Cu) composite, Appl. Phys. Lett. 99 (23) (2011) 232501, https://doi.org/10.1063/1.3665941.
[32] X.C. Zhong, H.C. Tian, S.S. Wang, Z.W. Liu, Z.G. Zheng, D.C. Zeng, Thermal, magnetic and magnetocaloric properties of $Fe_{80-x}M_xB_{10}Zr_9Cu_1$ (M = Ni, Ta; x= 0, 3, 5) amorphous alloys, J. Alloys Compd. 633 (2015) 188–193, https://doi.org/10.1016/j.jallcom.2015.02.037.
[33] H.C. Tian, X.C. Zhong, Z.W. Liu, Z.G. Zheng, J.X. Min, Achieving table-like magnetocaloric effect and large refrigerant capacity around room temperature in $Fe_{78-x}Ce_xSi_4Nb_5B_{12}Cu_1$ (x=0–10) composite materials, Mater. Lett. 138 (2015) 64–66, https://doi.org/10.1016/j.matlet.2014.09.127.
[34] G.F. Wang, Z.R. Zhao, X.F. Zhang, H.L. Li, G.P. Zhao, Peculiar effect of rare earth doping on magnetic and magnetocaloric properties in Fe-rich amorphous ribbons, J. Alloys Compd. 735 (2018) 104–108, https://doi.org/10.1016/j.jallcom.2017.11.025.
[35] Q. Wang, L.L. Pan, B.Z. Tang, D. Ding, L. Xia, Outstanding magnetocaloric properties at ambient temperature of a $Fe_{88}La_4Ce_3B_5$ amorphous alloy, J. Non-Cryst. Solids 580 (2022) 121394, https://doi.org/10.1016/j.jnoncrysol.2021.121394.
[36] M. Gao, L. Xie, Q. Li, J. Huo, C. Chang, Development of Fe-based amorphous alloy with high iron content for room-temperature magnetic refrigeration application, J. Appl. Phys. 132 (5) (2022) 055103, https://doi.org/10.1063/5.0098662.
[37] C. Xie, W. Li, F. Shen, Y. Liu, L. Xie, Z. Liao, S. Zhong, Plastic deformation behavior of a novel Fe-based metallic glass under different mechanical testing techniques, J. Non-Cryst. Solids.s 499 (2018) 58–61, https://doi.org/10.1016/j.jnoncrysol.2018.07.013.
[38] W. Yang, W. Li, C. Wan, J. Huo, J. Mo, H. Liu, B. Shen, Low-temperature magnetic properties and magnetocaloric effect of Fe–Zr–Cu amorphous alloys, J. Low Temp. Phys. 200 (1–2) (2020) 51–61, https://doi.org/10.1007/s10909-020-02452-z.
[39] T. Hashimoto, T. Numasawa, M. Shino, T. Okada, Magnetic refrigeration in the temperature range from 10 K to room temperature: the ferromagnetic refrigerants, Cryogenics 21 (11) (1981) 647–653, https://doi.org/10.1016/0011-2275(81)90254-X.
[40] K.A. Gschneidner, V.K. Pecharsky, Magnetocaloric materials, Annu. Rev. Mater. Sci. 30 (1) (2000) 387–429, https://doi.org/10.1146/annurev.matsci.30.1.387.
[41] A.P. Malozemoff, A.R. Williams, V.L. Moruzzi, Band-gap theory' of strong ferromagnetism: application to concentrated crystalline and amorphous Fe- and Co-metalloid alloys, Phys. Rev. B 29 (4) (1984) 1620–1632, https://doi.org/10.1103/PhysRevB.29.1620.
[42] B.D. Cullity, C. Dgraham, Introduction to Magnetic Materials, Wiley, 2009. ISBN: 9780471477419.
[43] K.A. Gallagher, M.A. Willard, V.N. Zabenkin, D.E. Laughlin, M.E. McHenry, Distributed exchange interactions and temperature dependent magnetization in amorphous $Fe_{88-x}Co_xZr_7B_4Cu_1$ alloys, J. Appl. Phys. 85 (8) (1999) 5130–5132, https://doi.org/10.1063/1.369100.
[44] K. Xu, H. Ling, Q. Li, J. Li, K. Yao, S. Guo, Effects of Co substitution for Fe on the glass forming ability and properties of $Fe_{80}P_{13}C_7$ bulk metallic glasses, Intermetallics 51 (2014) 53–58, https://doi.org/10.1016/j.intermet.2014.03.003.
[45] X. Moya, S. Kar-Narayan, N.D. Mathur, Caloric materials near ferroic phase transitions, Nature. Mater 13 (5) (2014) 439–450, https://doi.org/10.17863/CAM.13209.
[46] R. Zhu, X. Kan, X. Liu, M. Shezad, W. Wang, C. Liu, W. Yang, Z. Wang, Z. Chen, Magnetocaloric effect in Co-based amorphous alloy $Co_{90}Nb_{10}Ta_3$, J. Magn. Magn Mater. 484 (2019) 253–257, https://doi.org/10.1016/j.jmmm.2019.03.130.
[47] V.K. Pecharsky, K.A.G. Jr, Magnetocaloric effect and magnetic refrigeration, J. Magn. Magn Mater. 200 (1–3) (1999) 44–56, https://doi.org/10.1016/S0304-8853(99)00397-2.
[48] C. Liu, Q. Li, J. Huo, W. Yang, L. Chang, C. Chang, Y. Sun, Near room-temperature magnetocaloric effect of Co-based bulk metallic glass, J. Magn. Magn Mater. 446 (2018) 162–165, https://doi.org/10.1016/j.jmmm.2017.09.026.
[49] D.T.H. Gam, N.H. Hai, L.V. Vu, N.H. Luong, N. Chau, The existence of large magnetocaloric effect at low field variation and the anti-corrosion ability of Fe-rich alloy with Cr substituted for Fe, J. Phys.: Conf. Ser. 187 (2009) 012067, https://doi.org/10.1088/1742-6596/187/1/012067.
[50] J.Y. Law, R.V. Ramanujan, V. Franco, Tunable curie temperatures in Gd alloyed Fe–B–Cr magnetocaloric materials, J. Alloys Compd. 508 (1) (2010) 14–19, https://doi.org/10.1016/j.jallcom.2010.08.049.